

## Bleaching of sol-gel glass film with embedded gold nanoparticles by thermal poling

Francesco P. Mezzapesa, Isabel C. S. Carvalho,<sup>a)</sup> and Peter G. Kazansky  
*Optoelectronics Research Centre, University of Southampton, Southampton SO17 1 BJ, United Kingdom*

Olivier Deparis  
*Solid State Physics Laboratory, Physics Department, Facultés Universitaires Notre-Dame de la Paix,  
 B-5000 Namur, Belgium*

Mitsuhiro Kawazu and Koichi Sakaguchi  
*Technical Research Laboratory, Nippon Sheet Glass Co., Ltd., Itami, Hyogo 664-8520, Japan*

(Received 15 March 2006; accepted 27 September 2006; published online 3 November 2006)

Gold clusters embedded in glass are expected to be hard to dissolve in the form of ions since gold is essentially a nonreactive metal. In spite of that, bleaching of Au-doped nanocomposite sol-gel glass film on a soda-lime glass substrate is demonstrated in which electric-field thermal poling is employed to effectively dissolve randomly distributed gold nanoparticles (15 nm in diameter) embedded in a low conductivity sol-gel glass film with a volume filling factor as small as 2.3%. The surface plasmon absorption band at 520 nm is suppressed in the region covered by the anodic electrode. The phenomenon is explained by the ionization of the gold nanoparticles and the redistribution of gold ions in the glass matrix due to the action of the extremely high electrostatic field locally developed during poling. © 2006 American Institute of Physics.

[DOI: 10.1063/1.2382728]

Dielectric materials exhibiting surface plasmon resonances by inclusion of metallic nanometric-size clusters (nanoparticles) into their matrix have attracted, during the last decades, a considerable interest due to the unique flexibility in engineering their properties.<sup>1</sup> Optical properties of these nanocomposite materials are highly sensitive to the chemical composition of the nanoparticle (Ag, Au, Cu, etc.), the particle geometry (shape, size, etc.), the interface between the particle and the surrounding, and the topology of the particles, which all lead to selective optical absorption bands.<sup>2</sup> Surface plasmon polaritons and localized surface plasmons can be exploited in various near-field photonic devices,<sup>3</sup> such as in a resonantly excited metal nanoparticle plasmonic waveguide.<sup>4</sup> However, in order to develop practical devices, it is important to find ways to control the material properties. Recently, it has been shown that the surface plasmon resonance of silver<sup>5</sup> or copper<sup>6</sup> nanoparticles embedded in ion-conducting glasses could be bleached in a controlled way through electric-field-assisted dissolution of the embedded metallic clusters.

Gold is of great interest for the development plasmonic devices, either in the form of continuous, corrugated or perforated films<sup>3</sup> or in the form of nanoparticle chains or arrays.<sup>4</sup> In addition, the large optical Kerr nonlinearity of embedded gold nanoparticles<sup>7</sup> can be helpful for the development of light-controlled plasmonic devices. Recently, a way to control the size of gold nanoparticles at any location inside a glass host has been demonstrated through femtosecond-laser-induced dissolution of the nanoparticles.<sup>8</sup> From one side, an electric-field-assisted dissolution of embedded gold clusters should be significantly more difficult because gold as a metal is less easily oxidized than, e.g., silver, and gold ions (Au<sup>+</sup>) are less reactive in glass than silver ions (Ag<sup>+</sup>). This statement is supported, despite the

only slightly higher ionization potential of gold with respect to silver, by the fact that the standard reduction potential is +1.83 V for gold and +0.80 V for silver in aqueous solution,<sup>9</sup> but the data can be qualitatively applied to the case of solubility of metals and redox states of elements in glass. Another well known example is that silver can be dissolved into nitric acid (HNO<sub>3</sub>), which is known to be an oxidizing agent, whereas gold is not dissolved in HNO<sub>3</sub>. However, the response of embedded gold clusters to an electric-field-assisted dissolution experiment is difficult to predict for several reasons: detailed cluster interaction with the surrounding glass matrix depends on glass chemical composition, cluster size effects are important in chemical reactions (small gold clusters react differently than large ones); and the filling factor of metal clusters is important for determining the ionization conditions by the poling field.<sup>5</sup> Based solely on the fact that gold is essentially a nonreactive metal, it seems very hard to dissolve gold clusters embedded in glass.

In this letter, we demonstrate the dissolution of gold nanoparticles (15 nm in diameter) by dc electric field for a novel material design in which the nanoparticles were embedded in a high resistivity sol-gel film on top of a soda-lime-silicate glass substrate with a higher conductivity compared to the film. The resistivity and the thickness of the sol-gel film can be varied, introducing further control on the properties of the nanocomposite material which is useful for the development of future plasmonic devices.

A dielectric structure made of a low conductivity thin layer containing metal nanoparticles on an ion-conductive substrate is hereafter deliberately explored; more specifically, gold clusters are embedded in a sol-gel film on top of a soda-lime glass substrate. In spite of its larger thickness, the substrate is expected to be much less resistive than the thin film. With this structure, we demonstrate that gold nanoparticles can be dissolved by dc electric-field thermal poling only if specific conductivity conditions are satisfied.

<sup>a)</sup>Permanent address: Physics Department, PUC-Rio, 22453-900, Rio de Janeiro, Brazil; electronic mail: isabel@fis.puc-rio.br

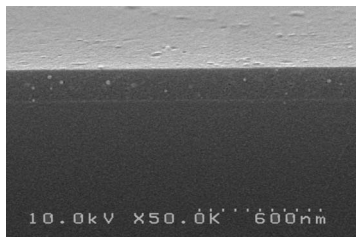


FIG. 1. SEM image of a pink sample (type 1): etched cross section (magnification: 50000 $\times$ , tilt angle: 10 $^\circ$ ). The gold nanoparticles can be seen as white spots randomly distributed in the 130-nm-thick sol-gel glass film.

The nanocomposite film was fabricated by the sol-gel method through the coating of a solution containing an organic silicon compound and a salt of gold onto a glass plate. As a result, the nanoparticles were randomly distributed within the film and no gradient of Au-particle concentration across the depth was observed when the scanning electron microscope (SEM) image of an etched sample cross section (Fig. 1) was examined. The film structure revealed nanoparticles uniformly dispersed in the matrix of silicate glass.

Two sets of 3-mm-thick substrates with different sol-gel film compositions (type 1 and type 2) were investigated, as summarized in Table I. The volume fractions of Au were estimated to be 2.3% and 5.2% and the Au-particle diameters were 15 and 8.5 nm for type 1 and type 2 samples, respectively. Iron oxide was also present in the substrates of type 1 (0.1 wt %) and type 2 (0.6 wt %) samples. According to the film composition, the samples were either pink (type 1) or blue (type 2) tinted, which is explained by the shift of the surface plasmon resonance towards the red with increasing host refractive index in these gold nanocomposite glasses,<sup>10</sup> as predicted by the Maxwell-Garnett effective medium theory.

Assuming the resistivity of the film ( $\rho_{\text{film}}$ ) being five orders of magnitude higher than that of the substrate ( $\rho_{\text{sub}}$ ), more than 80% of the applied voltage would drop across the film, i.e.,  $V_{\text{film}} = 1 / (1 + \rho_{\text{sub}} d_{\text{sub}} / \rho_{\text{film}} d_{\text{film}})$ , in spite of the fact that the ratio between the thicknesses of the film ( $d_{\text{film}}$ ) and the substrate ( $d_{\text{sub}}$ ) is as low as  $\sim 4.5 \times 10^{-5}$ .

In order to perform a comparative study on the two types of nanocomposite sol-gel film, both pink- and blue-colored samples were identically poled at 280  $^\circ\text{C}$  in air atmosphere by applying up to 1 kV through pressed-contact steel electrodes ( $9 \times 7 \text{ mm}^2$ ), with the sol-gel film surface facing the anode. The procedure used for poling soda-lime glass was employed<sup>11</sup> because of the high ionic conductivity of the

TABLE I. Characteristics of thin sol-gel films doped with Au nanoparticles.

Glass color	Refractive index	Sol-gel film composition	wt%	Film thickness (nm)
Pink (type 1)	1.46	SiO <sub>2</sub>	75.7	130
		TiO <sub>2</sub>	3.3	
		CeO <sub>2</sub>	5.0	
		Au	16.0	
Blue (type 2)	1.87	SiO <sub>2</sub>	19.5	140
		TiO <sub>2</sub>	25.9	
		CeO <sub>2</sub>	38.6	
		Au	16.0	

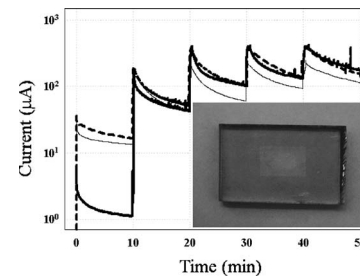


FIG. 2. Time evolution of the current during poling at 280  $^\circ\text{C}$  with the voltage increased in steps of 200 V (10 min each step) up to 1 kV (thick solid line: type 1 sample, thin solid line: type 2 sample). A type 1 sample was also poled with inverted polarity, i.e., with the film surface facing the cathode (dashed line). Inset: photograph of type 1 (pink) sample after poling at 280  $^\circ\text{C}$ , +1 kV. The bleached (i.e., colorless) region under the anode is well defined by the electrode size.

substrate. The voltage was increased in steps of 200 V for a fixed period of time (10 min each step). During each step, the current was limited in order to avoid runaway. When the final poling voltage was reached, the sample was cooled to room temperature while the voltage was applied.

The temporal evolution of the poling current (Fig. 2) can be understood in terms of ion depletion which takes place in the two-layer dielectric structure during poling. At the beginning of poling, the level of current in the pink sample was an order of magnitude lower than in a sample from the same batch poled with reverse polarity, i.e., with the film facing the cathode. This observation is in accordance with a lower resistivity of the bulk (substrate) relative to the sol-gel glass film. When the film faced the anode, there was no supply of cations from the anode (blocking electrode). Conversely, when the film faced the cathode the film could not block the movement of the cations (sodium ions, mainly) from the bulk. The asymmetry in the current evolution with respect to polarity was therefore explained by considering thermally activated cations injected from the bulk into the film, thus enhancing the conductivity of the film. Moreover, after the first voltage step, the current evolution in the pink sample trended towards the behavior of the inverted-poled pink sample. We interpreted this feature as an indication of film conductivity increase, which could be associated with the onset of Au nanoparticle dissolution.

Conductivity changes have already been reported for silver nanoparticle dissolution;<sup>5</sup> however, at high temperature the mobility of gold ions is expected to weakly contribute to the conductivity of the sol-gel layer in the present case. A possible explanation is the formation of defects in the sol-gel film, such as broken bonds, which could result in the increase of electron mobility. More interestingly, the blue sample followed behavior similar to the inverse-poled pink sample throughout the poling process, both in terms of current level and decay rate.

After poling, the film became colorless within the treated region of the pink sample well delimited by the anode geometry (see inset in Fig. 2): electric-field-assisted dissolution of gold nanoparticles took place. It was also verified that the pink color bleached when the film was chemically etched off. We speculate that, under the action of the high electrostatic field which developed in the sol-gel film during poling, ionization of the gold nanoparticles occurred with a subsequent migration of monovalent Au<sup>+</sup> ions into the glass substrate.

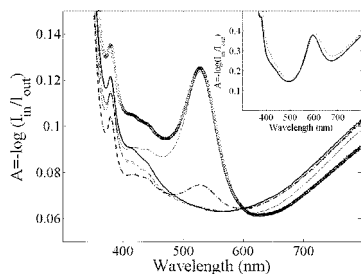


FIG. 3. Evolution of the optical absorbance spectrum of type 1 (pink) samples after poling with stepwise increasing voltage:  $5 \times 200$  V (thick solid line),  $4 \times 200$  V (dashed line),  $3 \times 200$  V (dashed-dotted line),  $2 \times 200$  V (thick dashed dotted line), and  $1 \times 400$  V (dotted line). The absorbance of the sample poled with reverse polarity (symbols) retraces the absorbance of the pristine sample (thin solid line) above 500 nm. Inset: absorbance spectra of the pristine (solid line) and 1 kV poled (dotted line) type 2 (blue) sample.

The measured absorbance spectra [ $A = -\log(I_{out}/I_{in})$ ] of unpoled and poled regions of the pink sample showed the suppression of the main absorbance band in the visible range after poling, as evidence of the bleaching effect (Fig. 3). The peak of the absorption band was located at 520 nm, as reported for surface plasmon resonance of such Au particles.<sup>12</sup> The absorption band centered at 376 nm was attributed to  $Fe^{3+}$  content in the host material. No change in the surface plasmon resonance could be measured after poling the pink sample with reversed polarity (with the film facing the cathode). This is not surprising, since the static electric-field ( $E_{dc}$ ) distribution induced by cation migration is localized under the anodic surface.

When the film faced the anode, one could estimate the value of  $E_{dc}$ , assuming, for simplicity, a uniform distribution across the 130 nm film thickness. By taking the smallest voltage value of 200 V,  $E_{dc}$  as high as  $1.5 \times 10^9$  V/m can be achieved. When compared with the electric field necessary to dissolve Ag particles embedded in glass ( $E_{dc} \cong 1$  kV/ $5 \mu\text{m} = 2 \times 10^8$  V/m from Ref. 5), the electric field evaluated for the dissolution of Au particles was higher by one order of magnitude. One reason for such a difference could be the much lower nanoparticle filling factor in the present samples, in comparison with the filling factor in the samples of Ref. 5.

Contrary to the observations in the pink sample, no bleaching could be reported in the blue sample after the treatment, although the poling conditions were kept identical; in the inset of Fig. 3 the absorbance spectra of the pristine and poled blue samples were compared. This striking difference in behavior of pink and blue samples is thought to be due to variations of resistivity and dielectric constant with the film composition. This allowed for a greater  $E_{dc}$  electric field to develop in the pink sample film under the same poling conditions.

The mechanism of gold cluster dissolution is as follows. In the presence of a high electric field, the cluster is ionized, electrons are ejected and extracted at the anode via tunneling from one cluster to the nearest one, and the positively charged gold ions are stripped off from the cluster by Coulomb forces and forward into the matrix leaving uncharged gold cluster behind.<sup>13</sup> This process could cycle until the cluster is totally destroyed and the gold ions are dissolved in the matrix. In this framework, the average distance between clusters could also influence the electronic conductivity via the potential barrier height for tunneling. The estimated fill-

ing fraction was 2.3% in the pink Au-doped sol-gel film, much lower than the reported value for the Ag-doped glass (tens of percent<sup>13</sup>), thus justifying the more intense electric-field strength required for gold dissolution.

Additional experiments were also performed in order to evaluate the voltage dependence for electric-field-assisted dissolution of gold nanoparticles. Pink samples were poled following the same poling procedure as described above but varying the final voltage (400 V, 600 V, 800 V, and 1 kV). Figure 3 shows the absorbance spectra measured as a function of final poling voltage. For a final voltage as low as 400 V, more than 50% reduction of the gold surface plasmon resonance was obtained, regardless of the number of voltage applied steps.

In conclusion, the demonstration of poling-assisted bleaching of Au-doped nanocomposite sol-gel film on top of ion-conducting glass substrate represents an important achievement in extending the bleaching of glasses with various compositions. A new sample structure is proposed; the sol-gel film with the embedded gold nanoparticles has a lower conductivity when compared with the high ionic conductivity of the soda-lime glass substrate. The resistivity and the thickness of the sol-gel film can be controlled providing a great versatility to the structure design. Along with the poling procedure, the sol-gel film composition was shown to play a crucial role in the dissolution process. Furthermore, by contrast to the previously reported results on silver nanoparticles, dissolution of gold nanoparticles was observed despite the much lower filling factor of nanoparticles. Finally, the perspective of being able to dissolve even less mobile particles embedded in thin films, such as platinum and palladium, broadens the application of poling-assisted bleaching towards optical device fabrication.

The authors are very grateful to Nippon Sheet Glass Co., Ltd. (NSG) in Japan for providing the samples. One of the authors (I.C.S.C.) acknowledges NSG for funding her Research Fellowship at the Optoelectronics Research Centre. K. Tanaka from Kyoto University is acknowledged for helpful discussions.

<sup>1</sup>K. L. Kelly, E. Coronado, L. L. Zhao, and G. C. Schatz, *J. Phys. Chem. B* **107**, 668 (2003).

<sup>2</sup>U. Kreibig and M. Vollmer, *Optical Properties of Metal Clusters* (Springer, Berlin, 1995), Chap. 4.

<sup>3</sup>A. V. Zayats and I. I. Smolyaninov, *J. Opt. A, Pure Appl. Opt.* **5**, S16 (2003).

<sup>4</sup>S. A. Maier, *Current Nanoscience* **1**, 17 (2005).

<sup>5</sup>O. Deparis, P. G. Kazansky, A. Abdolvand, A. Podliensky, G. Seifert, and H. Graener, *Appl. Phys. Lett.* **85**, 872 (2004); O. Deparis, P. G. Kazansky, A. Podliensky, A. Abdolvand, G. Seifert, and H. Graener, *ibid.* **86**, 261109 (2005).

<sup>6</sup>A. A. Lipovskii, V. G. Melehin, and V. D. Petrikov, *Tech. Phys. Lett.* **32**, 275 (2006).

<sup>7</sup>N. Pinçon-Roetzing, D. Prot, B. Palpant, E. Charron, and S. Debrus, *Mater. Sci. Eng., C* **19**, 51 (2002).

<sup>8</sup>X. Jiang, J. Qiu, H. Zeng, C. Zhu, and K. Hirao, *Chem. Phys. Lett.* **391**, 91 (2004).

<sup>9</sup>*Standard Potentials in Aqueous Solution*, edited by A. J. Bard, R. Parsons, and J. Jordan (Dekker, New York, 1985), pp. 318 and 310.

<sup>10</sup>T. Tsujino, M. Kawazu, and K. Maeda, *J. Sol-Gel Sci. Technol.* **19**, 852 (2000).

<sup>11</sup>F. C. Garcia, I. C. S. Carvalho, E. Hering, W. Margulis, and B. Lesche, *Appl. Phys. Lett.* **72**, 3252 (1998).

<sup>12</sup>R. H. Doremus, *J. Chem. Phys.* **40**, 2389 (1964).

<sup>13</sup>A. Podliensky, A. Abdolvand, G. Seifert, H. Graener, O. Deparis, and P. G. Kazansky, *J. Phys. Chem. B* **108**, 17699 (2004).